

Symmetrical Finite Element Model for Out-of-Plane Crushing of Nomex Honeycomb Structure

Wan Luqman Hakim Wan A Hamid^{1,*}, Mohd Sultan Ibrahim Shaik Dawood¹, and Yulfian Aminanda²

¹ Department of Mechanical and Aerospace Engineering, Kuliyah of Engineering, International Islamic University Malaysia, 53100 Gombak, Kuala Lumpur, Malaysia

² Faculty of Engineering, Universiti Teknologi Brunei, Jalan Tungku Link Gadong, BE1410 Brunei Darussalam

***Correspondence to:** Wan Luqman Hakim Wan A Hamid, Department of Mechanical and Aerospace Engineering, Kuliyah of Engineering, International Islamic University Malaysia, 53100 Gombak, Kuala Lumpur, Malaysia; Email: wanluqmanhakim@iium.edu.my

Abstract: The computational cost of Finite Element (FE) simulation of a honeycomb structure under compression is significantly high due to the large number of cell walls, frequent wall-to-wall contacts, and large deformations during loading. To address this, a symmetrical FE model was modelled and simulated to predict the crushing behaviour of a Nomex honeycomb under quasi-static axial compression, significantly reducing computational demand. The FE model's force-displacement response, crushing load (13.3 N), absorbed energy (69.6 mJ), and fold formation (9 folds) showed good agreement with experimental tests, confirming its reliability as a design tool. Beyond structural validation, this research demonstrates the potential of flexible honeycomb structures in aerospace applications, where their lightweight, energy-absorbing, and adaptive characteristics make them ideal for impact resistance, crashworthiness, and morphing components. By enabling efficient modelling and sustainable design, the study supports the advancement of aerospace structures that enhance safety, minimize resource consumption, and contribute to both wealth preservation and the protection of human life.

Keywords: Honeycomb structure; Out-of-plane crushing; Energy absorption; Finite Element Model (FEM) and Analysis (FEA)

1. Introduction

Honeycomb structures play a pivotal role in adaptive or morphing aerospace systems due to their unique combination of lightweight design, high stiffness-to-weight ratio, and inherent flexibility when properly engineered. Traditionally used as core materials in sandwich panels for aircraft wings, fuselages, and control surfaces, honeycombs

are now being adapted for dynamic applications where controlled deformation is required to alter the aircraft's shape or aerodynamic properties in real time. Extending beyond their conventional use, recent advances have transformed honeycombs from passive structural cores into active, deformable elements central to morphing airframe technologies.

Honeycomb structures, long valued for their



© The Author(s) 2025. **Open Access** This article is licensed under a Creative Commons Attribution 4.0 International License (<https://creativecommons.org/licenses/by/4.0/>), which permits unrestricted use, sharing, adaptation, distribution and reproduction in any medium or format, for any purpose, even commercially, as long as you give appropriate credit to the original author(s) and the source, provide a link to the Creative Commons license, and indicate if changes were made.

lightweight and high-stiffness characteristics in traditional aircraft components, have gained attention for applications in morphing and adaptive aerospace systems (Iannucci, 2012). Their ability to provide high out-of-plane rigidity while allowing in-plane flexibility makes them ideal for shape-changing mechanisms such as morphing wings and adaptive control surfaces (Zadeh *et al.*, 2020). Early studies focused on conventional Nomex and aluminium honeycombs used in sandwich structures for load-bearing yet lightweight components. However, traditional honeycombs lacked flexibility for the large deformations required in morphing systems. To overcome this limitation, researchers have explored flexible and re-entrant (auxetic) honeycomb geometries, which exhibit negative Poisson's ratios and enable smooth, controllable surface deformation (Lira *et al.*, 2009; Duncan *et al.*, 2018).

Building upon these developments, subsequent research moved beyond purely geometric modifications toward integrating multifunctional and adaptive materials within the honeycomb core itself. Further advancements introduced smart honeycomb materials, incorporating shape memory alloys, piezoelectric actuators, and pneumatic networks into the honeycomb core (Iannucci *et al.*, 2009). These systems enabled active stiffness control and programmed deformation, making it possible to modify camber, twist, or surface curvature (Ajaj *et al.*, 2018; Lachenal *et al.*, 2013). Studies by Olympio and Gandhi (2010) demonstrated morphing structures using hexagonal honeycomb reinforced with SMA actuation, achieving smooth, reversible shape transitions. Recently, 4D-printed and functionally graded honeycombs have been developed using materials such as shape-memory polymers and carbon-fiber composites (Xin *et al.*, 2020; Yue *et al.*, 2023). These allow programmable deformation paths and tunable stiffness, critical for next-generation UAVs and high-efficiency aircraft structures. Additionally, elastomer-skinned honeycomb cores were introduced to enhance aerodynamic smoothness during morphing (Chillara and Dapino, 2020).

While these innovations highlight the potential of smart and adaptive honeycombs, it is essential to first understand the fundamental mechanical role of conventional honeycomb cores in aerospace structures, particularly their contribution to stiffness and load-bearing efficiency. Honeycomb structures, commonly used as the core in sandwich panels, play a critical

role in resisting shear forces and enhancing bending stiffness. By increasing the distance between the top and bottom skins from the neutral axis, the honeycomb core effectively amplifies the second moment of area, enabling the sandwich structure to withstand greater bending moments. This configuration imparts one of the defining characteristics of sandwich structures: exceptionally high specific flexural stiffness and flexural strength. As a result, a sandwich panel can sustain significantly higher bending loads compared to a solid plate of similar dimensions and weight, making it a superior choice for lightweight yet high-strength aerospace applications.

Nomex honeycomb is a lightweight core material widely used in aerospace composite structures due to its excellent strength-to-weight ratio, fire resistance, and energy absorption capabilities. It is made from aramid fibre paper (Nomex) impregnated with phenolic resin and formed into a hexagonal cell structure, which provides high stiffness and compressive strength while keeping weight to a minimum. Nomex honeycomb is commonly used as the core in sandwich composite panels, where it is bonded between carbon fibre or glass fibre face sheets. This configuration offers high flexural rigidity and resistance to bending, crucial for aircraft components such as wings, fuselage panels, floors, doors, and control surfaces. Because weight reduction is essential for fuel efficiency and payload optimization in aircraft, Nomex honeycomb offers a superior alternative to solid laminates or metal structures. Nomex material is naturally flame-retardant and maintains structural integrity at elevated temperatures, which is vital for aircraft cabin interiors, engine nacelles, helicopter blades, and radomes. Nomex honeycomb efficiently absorbs impact energy, making it ideal for crashworthy structures, helicopter landing gear fairings, leading-edge surfaces, and protective panels. Unlike aluminum honeycomb, Nomex is corrosion-resistant and maintains durability under cyclic loading, reducing maintenance needs over the aircraft's service life.

The honeycomb core of sandwich structures can be subjected to a compression load (e.g. payload on the sandwiched floor panel of an aircraft, seat and passengers weight, food cart, etc.) and it can be crushed if it is excessively loaded (i.e. excessive payload, heavy luggage, oversized passengers, etc.). To model and simulate the crushing of the entire honeycomb structure

subjected to the compression load, the computational cost is extremely high due to the large numbers of honeycomb walls and large deformation. Hence, some researchers used robust finite element model by utilising a series of non-linear springs to simulate the compression and deformation of the honeycomb structures (Aminanda *et al.*, 2005). Even though a honeycomb material model is currently available (LSTC, 2015) to predict the honeycomb behaviour, it is only suitable for a structure modelled with solid elements, which does not significantly solve the main issue of high computational cost. Moreover, the solid elements do not appropriately represent the honeycomb structure, because in reality, the honeycomb structure consists of tens or hundreds of thin-walled plates and hollow honeycomb cells.

Aluminum and Nomex honeycomb cores have been extensively utilized in aerospace and engineering structures because of their exceptional lightweight characteristics, high energy absorption, and inherent fire resistance. The axial crushing behaviour of aluminium honeycombs was first investigated by McFarland (1963) and later refined by Wierzbicki (1983), who identified folding and rolling of the cell walls as the primary deformation mechanisms during out-of-plane compression. These deformation modes were subsequently validated by Zhang and Ashby (1992) through analytical and experimental studies on honeycombs composed of plastic-rigid materials. Further experimental investigations by Wu and Jiang (1997) on six types of aluminium honeycombs demonstrated that the crushing strength and buckling wavelength predicted by Wierzbicki's theoretical model, and by manufacturer-provided data, were underestimated when compared with actual test results, underscoring the need for more accurate predictive models for cellular structure behaviour under axial compression.

The crushing behaviour of Nomex honeycomb structures was investigated by Aminanda *et al.* (2005) through a combination of experimental observation and modelling. Based on phenomenological observations using a paper-based honeycomb model, the researchers hypothesized that the majority of the compressive load is carried by the vertical edges of the honeycomb cells, as buckling of the cell walls typically occurs prior to the failure of these vertical members. Consequently, the honeycomb under axial compression was

represented as a grid of nonlinear springs, with each spring's behaviour derived directly from the force-displacement response of an individual vertical edge. This simplified yet physically meaningful modelling approach effectively captured the structural response of the honeycomb. The model was subsequently validated through indentation tests on Nomex honeycombs, demonstrating a strong correlation between the experimental results and the finite element (FE) predictions based on the nonlinear spring network (Aminanda *et al.*, 2005; Castanié *et al.*, 2008).

Building on these foundational insights into the compressive response of Nomex cores, later studies expanded the investigation to include material reinforcement effects and comparative modelling approaches for metallic and composite honeycombs. Tiwari *et al.* (2018) investigated the effect of reinforcement within aluminium honeycomb structures and reported that increasing reinforcement led to a rise in the material's relative density and, consequently, a noticeable improvement in crushing strength. In their analysis, the authors also referred to established theoretical models proposed by Wierzbicki *et al.* (1983), which are often used for predicting the crushing behaviour of honeycomb structures based on a single Y-shaped unit cell (Wierzbicki *et al.*, 1983; Wu & Jiang, 1997). The present paper, which summarizes part of a broader study (Wan A Hamid, 2014), builds upon this understanding by proposing a symmetrical finite element (FE) model to predict the crushing behaviour of Nomex honeycomb structures under axial compression. Unlike the theoretical Y-cell approximation, the FE model captures the response of multiple cells, including the formation of folds, energy absorption and deformation mechanisms, thus offering a more comprehensive approach to honeycomb crushing simulation.

This modelling strategy is not limited to Nomex honeycombs; rather, it can be generalized to a broad range of cellular architectures and material systems through appropriate adaptation of geometric and constitutive parameters. By modifying the unit cell topology (Wang *et al.*, 2022), such as hexagonal, square, triangular, or re-entrant (auxetic) geometries, the model can simulate diverse deformation modes, including progressive folding, localized buckling, and shear band propagation, which are characteristic of different honeycomb and lattice structures. The symmetry-based reduction technique, which

minimizes computational cost while preserving essential deformation characteristics, can also be extended to irregular or graded cellular designs, where the mechanical response varies spatially across the structure. This makes the approach highly adaptable for investigating functionally graded or hierarchical honeycombs increasingly used in aerospace and energy-absorbing applications.

Similarly, the modelling framework can be expanded to incorporate various material constitutive laws, ranging from linear-elastic and elastic-plastic metals (such as aluminium and titanium alloys) to viscoelastic polymers, fibre-reinforced composites, and even smart materials such as shape memory alloys (SMAs) (Wan A Hamid *et al.*, 2020) or piezoelectric composites. Through the integration of appropriate material models, for example, elasto-plastic, damage-based, or temperature-dependent formulations, the FE model can replicate both rate-dependent and thermomechanical effects, enabling more accurate prediction of crushing and energy absorption across different operational environments. Furthermore, the methodology can be adapted to simulate dynamic impact loading (Xia *et al.*, 2023), multi-axial stresses, or out-of-plane bending, which are often encountered in aerospace structures under crash, landing, or morphing conditions. The combination of symmetry reduction, detailed contact interaction, and flexible material modelling thus provides a generalizable, computationally efficient framework for studying the mechanical response of a

wide range of cellular materials, from metallic foams and lattice metamaterials to bio-inspired composites, under complex loading conditions.

2. Finite Element Model of Thin-Walled Honeycomb Structure

In the two-dimensional perspective, the symmetry of the honeycomb structure about its principal symmetry axes (indicated by red dashed lines) is illustrated in **Fig. 1**. Each hexagonal cell can be divided into six identical symmetrical segments, represented by six dotted triangular regions. Within each segment, or symmetrical model, the geometry comprises one double-thickness horizontal wall and two single-thickness inclined walls. In the three-dimensional model, **Fig. 2a** shows a finite element (FE) representation of seven interconnected honeycomb cells, where each of the six symmetrical models is highlighted in a different colour. **Fig. 2b** presents a single symmetrical FE model. Both the full honeycomb structure and the symmetrical model are developed using 3D continuum shell elements. Regarding the geometrical specifications, the honeycomb structure has a cell size of 3.2 mm and a corresponding cell diameter of 4.2 mm. The double-thickness horizontal walls and single-thickness inclined walls have lengths of 1.8 mm and 2.0 mm, respectively. For the symmetrical model, these lengths are halved to 0.9 mm and 1.0 mm. The height (thickness) of the honeycomb and the symmetrical model is consistent at 11.9 mm.

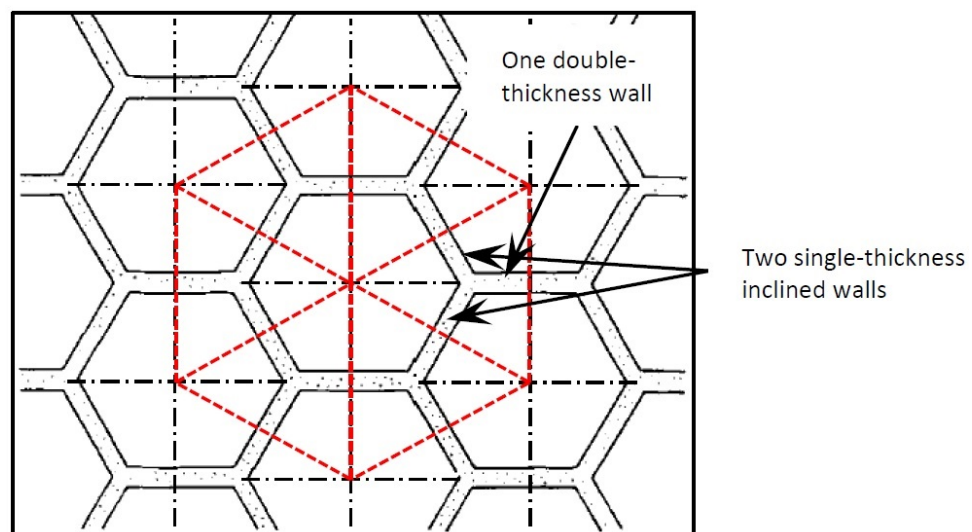


Figure 1. Symmetrical geometry of honeycomb structure.

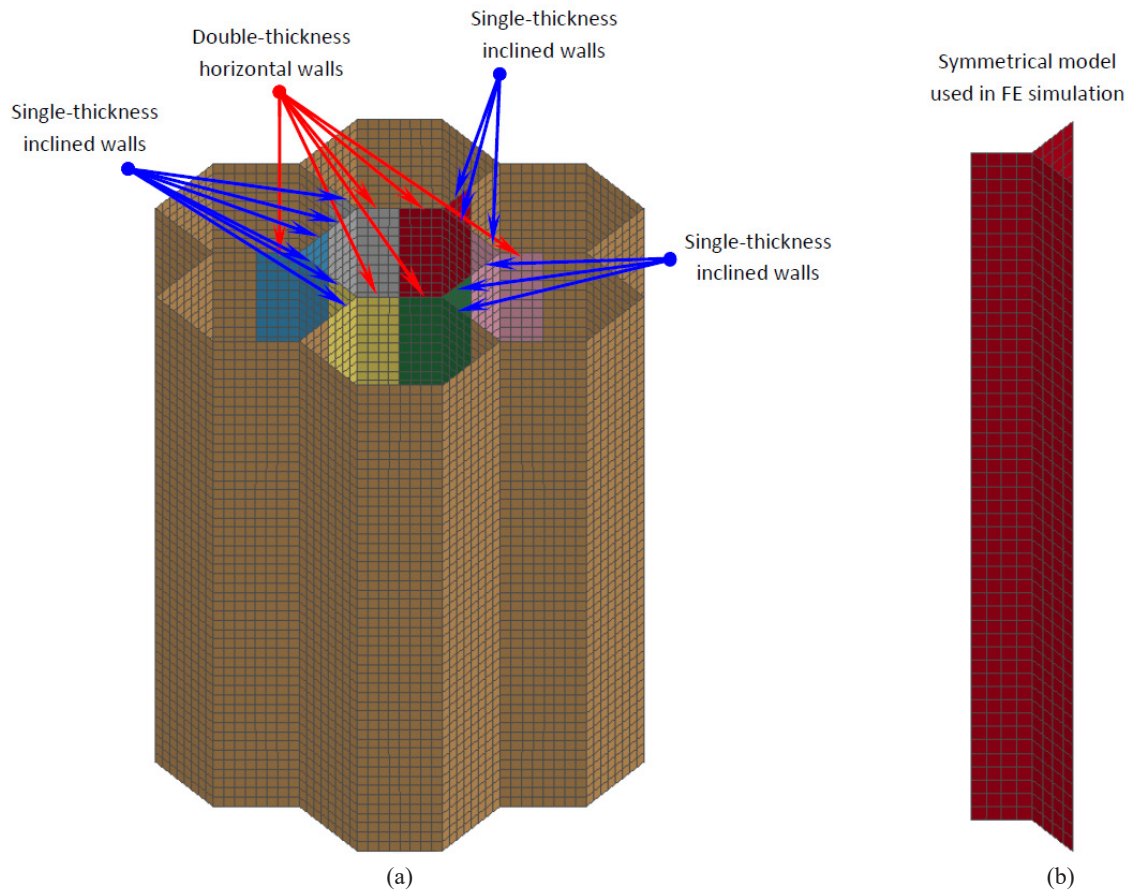


Figure 2. (a) Position of symmetrical models in a honeycomb structure and (b) a symmetrical model used in FE simulation.

In the symmetrical finite element (FE) model, each horizontal and inclined wall was discretised using 200 shell elements (4 elements \times 50 elements), corresponding to an approximate element size of 0.2 mm. To ensure proper constraint and realistic deformation behaviour, the nodes along the bottom edges of the model were fully fixed in all degrees of freedom. Meanwhile, the nodes along the lateral edges were constrained so that they could only translate within a plane perpendicular to the respective wall, allowing realistic deformation while preventing unwanted rigid-body motion.

A Piecewise Linear Plasticity material model was applied to all components of the Honeycomb structure. The assigned material properties are listed in **Table 1**:

Table 1: Material properties of Nomex honeycomb.

Material Properties	Values
Density	$9.66 \times 10^{-7} \text{ kg/mm}^3$
Elastic Modulus	1.218 GPa
Yield Stress	62.9 MPa
Poisson's Ratio	0.25
Tangent modulus	0.1 GPa

Loading was applied via a rigid compression plate, positioned above the FE model (not shown), and displaced in the downward (z) direction at a rate of 35.7 mm/min, corresponding to a strain rate of approximately 0.05 s^{-1} . To accurately capture the interaction between elements during crushing, two contact definitions were implemented; (1) single surface contact for self-contact between elements of each wall, and (2) surface-to-surface contact between the horizontal and inclined walls, and between the compression plate and the honeycomb structure.

Fig. 3 presents the buckling and post-buckling behaviour of the symmetrical FE model of the Nomex honeycomb structure. The crushing progression is shown in both isometric and front views, captured at 1.5-second time intervals, and correlated with the corresponding points on the force-time history curve. In the visual (**Fig. 3a and 3b**), within the model, the double-thickness horizontal wall is depicted in dark brown, while the two single-thickness inclined walls are shown in light brown, allowing clear visual differentiation of the deformation patterns. The analysis

reveals that initial buckling occurs at a compression load of approximately 13.2 N. Following this first buckling event, the double-thickness horizontal wall undergoes progressive folding, and by 15 seconds, a total of eight distinct folds are observed. Throughout this period, the structure exhibits a relatively stable

plateau force of about 9 N, characteristic of the energy-absorbing phase of cell wall deformation. As deformation continues, the system transitions into the densification stage, where the cell walls fully collapse and the force increases sharply due to material drastically increased material compaction.

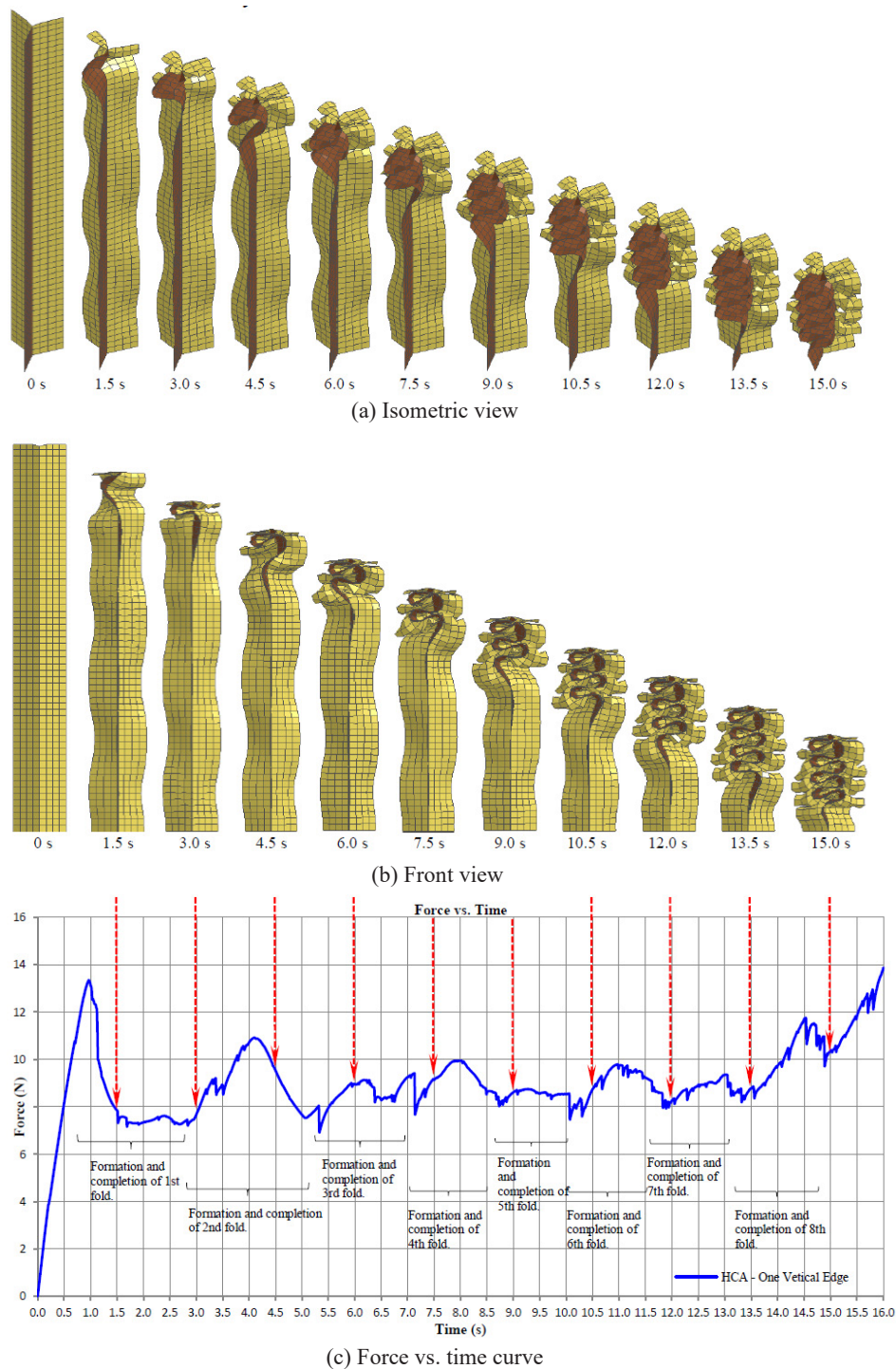


Figure 3. Folding mechanism of a symmetrical FE model of Nomex honeycomb structure; (a) isometric view, (b) front view, and (c) associated force vs. time curve.

The data from the FE analysis, both the reaction forces from the fixed bottom end and the vertical displacement of the loading top side, were extracted and processed. This information was then plotted to produce a force-displacement (F-D) curve, which was used as a basis for comparison with the experimental results. This comparison is presented later in the validation section to assess the accuracy of the FE model.

3. Experimental Out-of-Plane Quasi-Static Compression Test

A series of quasi-static out-of-plane compression tests were conducted on Nomex honeycomb specimens to evaluate their crushing behaviour. Each specimen had a height of 11.9 mm, a cell size of 3.2 mm, a wall thickness of 0.1 mm, and consisted of 77 hexagonal cells with 190 symmetrical sections. To ensure accuracy and repeatability, three specimens were tested

under identical conditions. The tests were performed using an INSTRON universal testing machine, with the bottom platen fixed and the top platen applying a vertical downward displacement. The experimental setup is shown in **Fig. 4**. A displacement rate of 35.7 mm/min was applied, corresponding to a strain rate of 0.05 s^{-1} . During testing, the compressive force was recorded using a load cell, while the vertical displacement of the upper crosshead was continuously monitored. The resulting force-displacement curves were plotted, as illustrated in **Fig. 5**. The Nomex honeycombs exhibited an average crushing load of 2.9 kN. The total energy absorbed, calculated from the linear elastic region through the plateau region up to just before densification, was approximately 17 J. The conditions of the specimens before and after testing are shown in **Fig. 6**, demonstrating the characteristic progressive folding behaviour under compression.

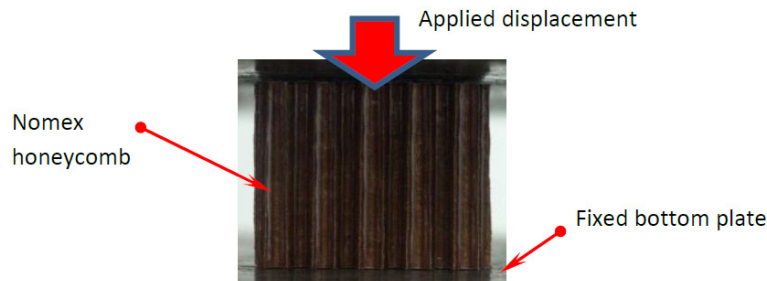


Figure 4. Experimental setup of Nomex honeycomb structure subjected to quasi-static compression load.

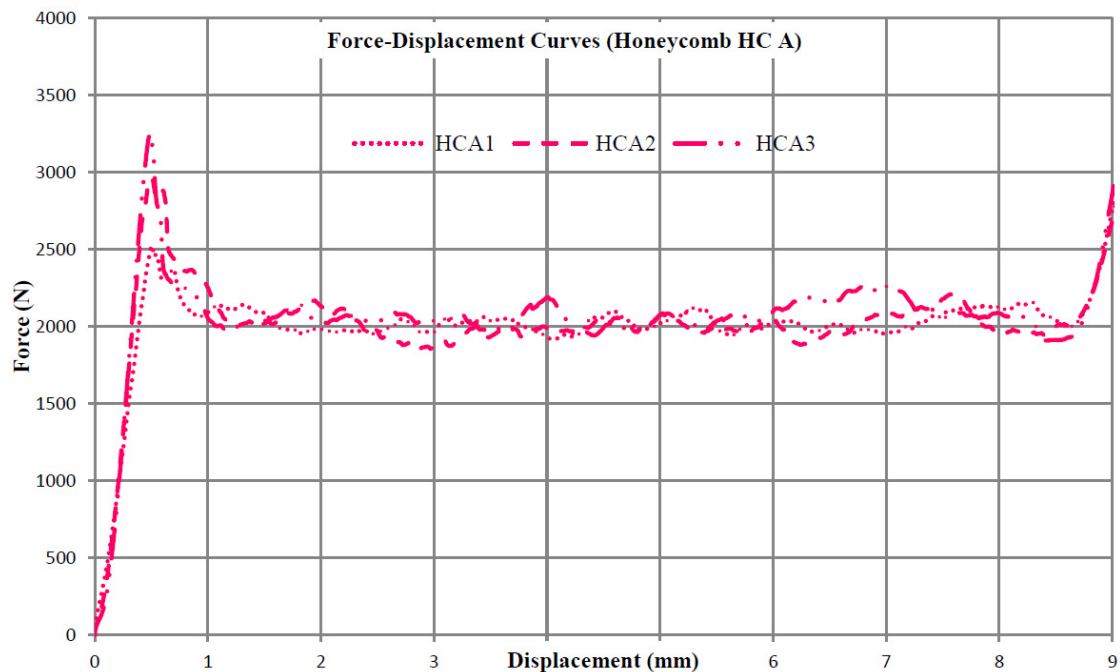


Figure 5. Experimental force-displacement curves of Nomex honeycomb structure subjected to out-of-plane crushing.

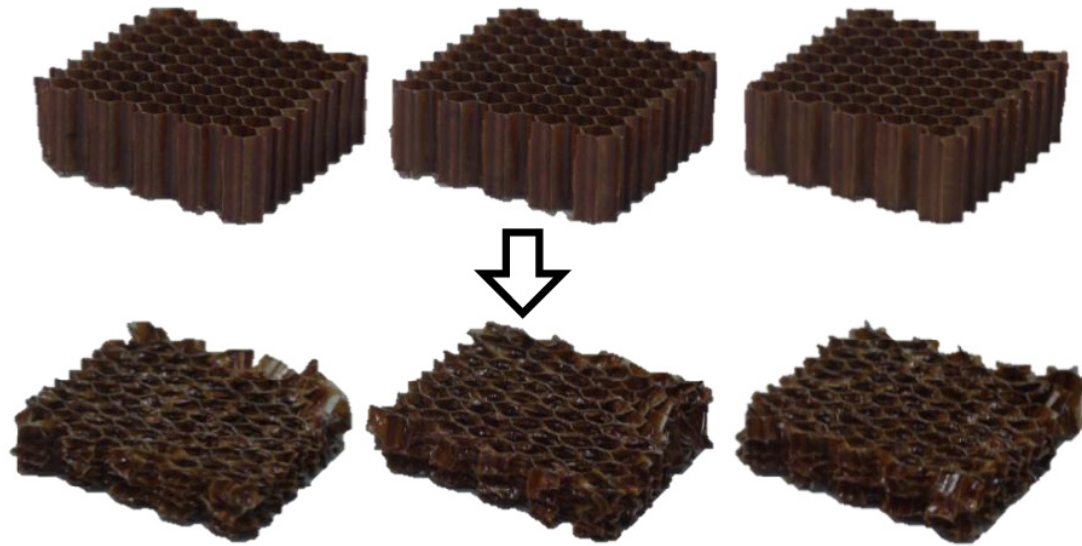


Figure 6. Nomex honeycombs before (top) and after (bottom) out-of-plane quasi static compression tests.

The quasi-static compression tests clearly demonstrate the typical three-stage crushing behaviour of Nomex honeycomb structures: an initial linear elastic region, a plateau region characterized by progressive folding, and a final densification stage. The average crushing load of 2.9 kN indicates that the specimens possess a strong out-of-plane load-bearing capacity relative to their low mass, affirming the high specific strength of Nomex honeycomb cores. The energy absorption of approximately 17 J reflects the material's excellent capability to dissipate mechanical energy through sequential cell wall buckling and collapse, which is an essential feature for impact and crashworthy aerospace structures.

The close consistency among the force-displacement curves of the three specimens confirms the repeatability and reliability of the experimental procedure. The force-displacement curves (**Fig. 5**) exhibit a well-defined plateau, signifying stable plastic deformation and controlled progressive folding rather than brittle failure. Visual inspection of the post-test specimens (**Fig. 6**) reveals uniform fold formation and layer-by-layer collapse, which aligns with classical honeycomb crushing behaviour observed in prior studies (e.g., Wierzbicki, 1983; Wu & Jiang, 1997). Overall, the results validate that Nomex honeycomb maintains predictable and energy-efficient deformation under axial compression, making it highly suitable for lightweight structural applications where impact resistance and energy absorption are critical.

4. Validation of Symmetrical FE Model of Honeycomb Structure by Experimental Test

The force-displacement (FD) curve obtained from the finite element (FE) simulation on the symmetrical FE model of Nomex honeycomb structure is compared with the FD curve obtained from the quasi-static experimental test, as depicted in **Fig. 7**. The red solid line is the experimental FD curve, and the blue dotted line is the FE FD curve. We found that the peak forces were close, but the FE plateau force was lower than the experimental plateau force. The experimental and FE peak forces were 13.28 N and 13.32 N, respectively, which were extremely close, with only 0.3% percentage difference. The energy absorbed were 89.10 mJ and 69.57 mJ, respectively, for a symmetrical model/section. Lower plateau force obtained from the FE simulation resulted in lower energy absorption, thus higher percentage difference (21.9%). The difference was believed due to the selection of linear-plasticity material model for the symmetrical FE model instead of the real brittle properties of Nomex honeycomb structure. However, the proposed material gave a quite reasonable comparison in term of the peak force. Another factor contributed to the difference in the plateau force was adhesive. No adhesive material was modelled for the double-thickness wall of the symmetrical FE model. In contrast, adhesive existed between the walls of the double-thickness section of Nomex honeycomb structure used in the experimental tests. The additional adhesive material may increase the shear resistance between the walls of multiple double-thickness sections, and

consequently increased the plateau force during crushing of the honeycomb structure. Comparison of the crushing

properties of the Nomex honeycomb structure are summarised in **Table 2**.

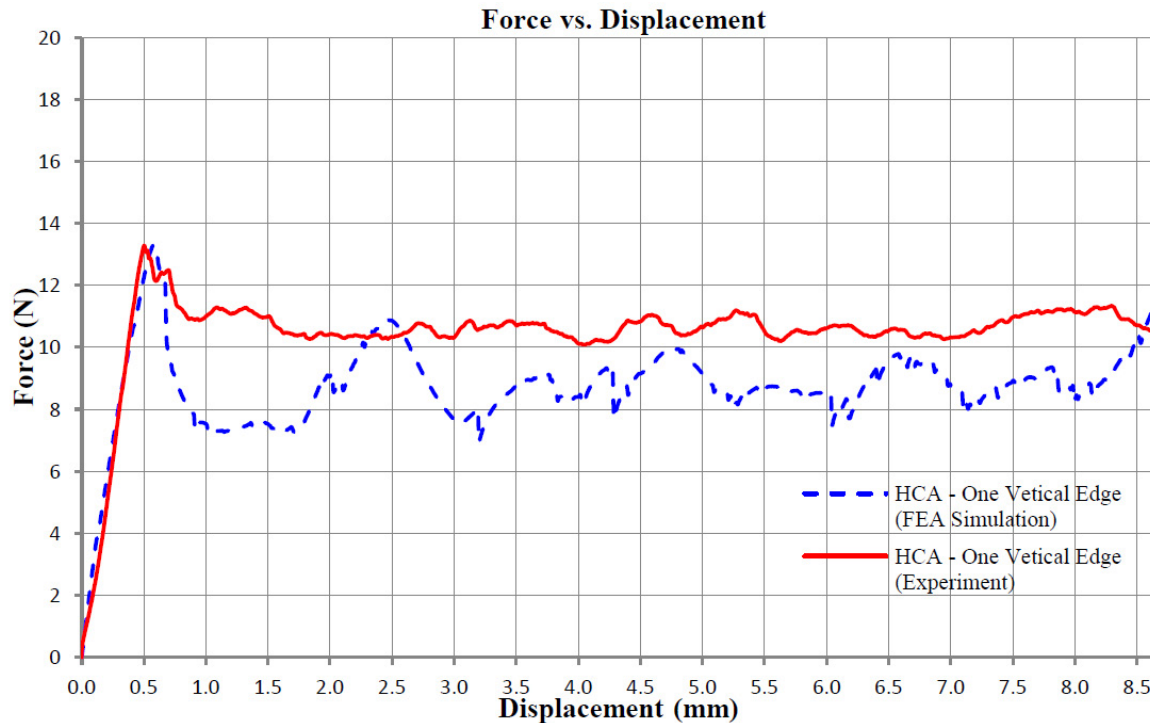


Figure 7. Comparison of force-displacement curves between experimental test and LS-DYNA simulation for Nomex honeycomb (HCA).

The FE model produces the peak crushing force very well: experimental peak = 13.28 N, FE peak = 13.32 N (difference $\approx 0.3\%$). This excellent match indicates the FE geometry, boundary conditions, contact setup and the selected stiffness in the initial loading regime capture the elastic response and onset of collapse accurately. However, the FE plateau force is lower than the experimental plateau, producing lower absorbed energy in the simulation (FE energy = 69.57 mJ, experiment = 89.10 mJ for the symmetrical section), with a 21.9% difference in energy. Because most energy in cellular crushing is accumulated across the plateau region, the plateau mismatch dominates the energy discrepancy.

The FE used a linear-plastic material representation while the real Nomex paper/phenolic honeycomb behaves in a brittle, damage-dominated manner (micro-fracture, delamination, fiber pull-out). Linear-plastic models tend to under predict local stiffness/strength during progressive folding and cannot capture sudden local fractures that increase resistance during plateau crushing. The experimental honeycomb contains adhesive

between double-thickness walls and junctions, in contrast the FE model did not include this adhesive. Adhesive layers increase shear transfer between adjacent walls and stabilise fold formation, raising the plateau resistance and thus the absorbed energy. Actual crushing involves crack initiation, propagation, frictional sliding and contact between folded faces. Simplified contact/friction parameters or omission of cohesive/fracture models, can reduce the simulated resistance during folding.

Real honeycomb specimens contain voids, local thickness variations and imperfect bonding. These features can either reduce or sometimes increase plateau resistance depending on distribution. If the experimental specimen had beneficial bonding patterns, the experimental plateau could be higher than an idealised FE model. Coarse meshes or insufficient contact element resolution at folding regions can smooth sharp local behaviour and underestimate local bending/crushing resistance. Although tests were quasi-static, the numerical algorithm's damping, mass scaling, or inconsistent rate effects in the material model can influence energy dissipation in the plateau.

Table 2. Comparison of peak forces and energy absorption capability between experimental test and LS-DYNA simulation for Nomex honeycomb structure.

Nomex Honeycomb	Experimental Test				LS-Dyna Simulation (A Symmetrical Model)		% Difference	
	190 Vertical Edges / Symmetrical Section		One Vertical Edge (One Symmetrical Section)		Peak Force(N)	Energy Absorbed (mJ)	Peak Force	Energy Absorbed
	Peak Force(N)	Energy Absorbed (J)	Peak Force(N)	Energy Absorbed (mJ)				
HCA1	2524	16.93	13.28	89.10	13.32	69.57	0.30	21.92

A comparison was also conducted based on the deformation patterns of a single symmetrical section of the Nomex honeycomb structure. The FE simulation predicted the development of nine distinct folds in the double-thickness cell walls during out-of-plane compression. In the experimental tests, however, the number of folds ranged from 9 to 13, indicating a slight variability across specimens. This variation is likely due to factors such as non-uniformity in material density, cell wall thickness, adhesive distribution, and local defects introduced during the manufacturing of the Nomex honeycomb. Despite this variation, the simulated result is considered highly acceptable because the predicted number of 9 folds falls within the observed experimental range. Additionally, the formation of more folds in some experimental specimens helps explain the somewhat higher plateau force and energy absorption seen in the experimental force–displacement curves compared to the FE simulation. As more folds form, additional work is required for each successive buckling and crushing event, resulting in increased energy absorption and a higher sustained plateau load. **Fig. 8** shows a side-by-side comparison of the fold formation captured in both the experimental test and the numerical simulation, where the characteristic nine-fold deformation pattern is evident.

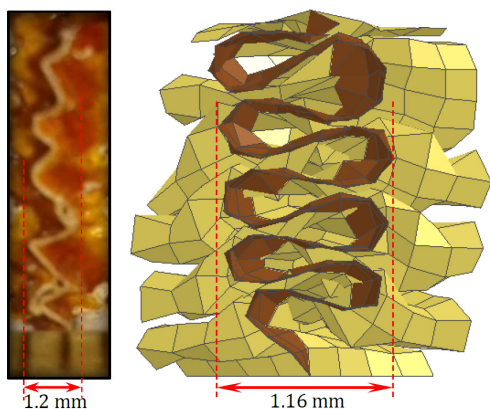


Figure 8. Comparison between experimental and LS-DYNA simulation results on fold formation of double-thickness horizontal wall.

In future work, incorporating damage and cohesive behaviour into the FE model will enhance its predictive accuracy, particularly in capturing the plateau region and energy absorption characteristics. Two promising approaches are the cohesive zone model (CZM) for interfacial and adhesive regions, and continuum damage mechanics (CDM) for modelling the degradation of cell wall material. Implementing cohesive elements or cohesive surface interactions at the double-thickness wall interfaces, where adhesive layers exist in the actual Nomex honeycomb, would allow the simulation to capture damage initiation, progressive debonding, and interfacial shear transfer, thereby improving the representation of energy dissipation during crushing. In parallel, adopting a damageable constitutive model for the Nomex paper/phenolic cell walls, treated as brittle or quasi-brittle materials, would enable the model to reproduce stiffness degradation, micro-cracking, and post-buckling softening through a scalar or tensor-based damage variable. Together, these enhancements would provide a more physically realistic depiction of the crushing process, bridging the gap between numerical predictions and experimental observations.

5. Conclusion

A symmetrical finite element (FE) model of a Nomex honeycomb core was developed and subjected to out-of-plane quasi-static compression, with its force–displacement response validated against experimental results. The simulation predicted a crushing load of 13.3 N and energy absorption of 69.6 mJ, while exhibiting nine progressive folds during the crushing process, closely matching the 9–13 folds observed experimentally. The strong correlation between the numerical and experimental outcomes in terms of peak load, energy dissipation, and deformation pattern demonstrates that the proposed symmetrical FE model provides a robust and reliable tool for predicting the structural response of Nomex honeycomb cores under out-of-plane loading. This modelling framework not

only captures the essential crushing mechanics with high fidelity but also establishes a solid foundation for future extensions incorporating damage evolution and cohesive interactions, enabling more comprehensive simulations of cellular material behaviour under complex loading conditions.

References

- [1] Ajaj R.M. and Jankee G.K. (2018) The transformer: A multimission UAV capable of symmetric and asymmetric span morphing, *Aerospace Science and Technology*.
- [2] Aminanda Y., Castanié B., Barrau J.J. and Thevenet P. (2005) Experimental analysis and modeling of the crushing of honeycomb cores, *Applied Composite Materials*, vol. 12, pp. 213-227.
- [3] Castanié B., Bouvet C., Aminanda Y., Barrau J.J. and Thevenet P. (2008) Modelling of low energy/low velocity impact on Nomex honeycomb sandwich structures with metallic skins, *International Journal of Impact Engineering*, vol. 35, issue 7, pp. 620-634.
- [4] Chillara V.S.C. and Dapino M.J. (2020) Review of morphing laminated composites, *Applied Mechanics Reviews, Transactions of the ASME*, vol. 72.
- [5] Duncan O., Shepherd T., Moroney C., Foster L., Venkatraman P.B., Winwood K., Allen T. and Alderson A. (2018) Review of auxetic materials for sports applications: Expanding options in comfort and protection, *Applied Sciences*, 8, 941.
- [6] Iannucci L. (2012) Aerofoil member, US-Patent No. 8,186,631.
- [7] Iannucci L., Evans M., Irvine R., Patoor R. and Osmont D. (2009) Morphing wing design, *MCM-ITP Conference*, Lille - Grand Palais.
- [8] Lachenal X., Daynes S. and Weaver P.M. (2013) Review of morphing concepts and materials for wind turbine blade applications, *Wind Energy*, 16, 283-307.
- [9] Lira C., Innocenti P. and Scarpa F. (2009) Transverse elastic shear of auxetic multi re-entrant honeycombs, *Composite Structures*, 90, 314-322.
- [10] Livermore Software Technology Corporation (LSTC) (2015) LS-DYNA Keyword User's Manual, Volume II Material Models, Version R8.0.
- [11] McFarland R.K. Jr. (1963) Hexagonal cell structures under post-buckling axial load, *AIAA Journal*, vol. 1, no. 6, pp. 1380-1385.
- [12] Olympio K.R. and Gandhi F. (2010) Zero Poisson's ratio cellular honeycombs for flex skins undergoing one-dimensional morphing, *Journal of Intelligent Material Systems and Structures*, 21(17), pp. 1737-1753.
- [13] Tiwari G., Thomas T. and Khandelwal R.P. (2018) Influence of reinforcement in the honeycomb structure under axial compressive load, *Thin-Walled Structures*, vol. 126, pp. 238-245.
- [14] Wan A Hamid, W.L.H. (2014) Experimental and simulation study of energy absorption capability of foam-filled Nomex honeycomb structure, *Master Thesis*, International Islamic University Malaysia.
- [15] Wan A Hamid W.L.H., Iannucci L. and Robinson P. (2020) Finite-element modelling of NiTi shape-memory wires for morphing aerofoils, *The Aeronautical Journal*, vol. 124, 1281, 1740-1760.
- [16] Wang S., Xia H. and Liu Y. (2022) Energy absorption characteristics of polygonal bio-inspired honeycomb column thin-walled structure under quasi-static uniaxial compression loading, *Biomimetics*, 7, 201.
- [17] Wierzbicki T. (1983) Crushing analysis of metal honeycombs, *International Journal of Impact Engineering*, vol. 1, no. 2, pp. 157-174.
- [18] Wu E. and Jiang W.-S. (1997) Axial crush of metallic honeycombs, *International Journal of Impact Engineering*, vol. 19, nos. 5-6, pp. 439-456.
- [19] Xia H., Sun Q. and Wang S. (2023) Influence of strain rate effect on energy absorption characteristics of bio-inspired honeycomb column thin-walled structure under impact loading, *Case Studies in Construction Materials*, 18, e01761.
- [20] Xin X., Liu L., Liu Y. and Leng J. (2020) Origami-inspired self-deployment 4D printed honeycomb sandwich structure with large shape transformation, *Smart Materials and Structures*, 29, 065015.
- [21] Yue C., Zhao W., Li F., Liu L., Liu Y. and Leng J. (2023) Shape recovery properties and load-carrying capacity of a 4D printed thick-walled kirigami-inspired honeycomb structure, *Bio-Design and Manufacturing*.

- [22] Zadeh M.N., Dayyani I. and Yasaee M. (2020) Fish Cells, a new zero Poisson's ratio metamaterial – Part I: Design and experiment, *Journal of Intelligent Material Systems and Structures*, vol. 31 (13), pp. 1617-1637.
- [23] Zhang J. and Ashby M.F. (1992) The out-of-plane properties of honeycombs, *International Journal of Mechanical Sciences*, vol. 34, no. 6, pp. 475-489.